Inorganic Chemistry

Article

pubs.acs.org/IC

Rigid, Perdeuterated Lanthanoid Cryptates: Extraordinarily Bright Near-IR Luminophores.

Christine Doffek,[†] Nicola Alzakhem,[†] Mariusz Molon,[‡] and Michael Seitz*,[†]

[†]Inorganic Chemistry I and [‡]Inorganic Chemistry II, Department of Chemistry and Biochemistry, Ruhr-University Bochum, 44780 Bochum, Germany

Supporting Information

ABSTRACT: Near-IR emissive lanthanoid cryptates have been developed with the lanthanoids Yb, Nd, Er, and Pr by designing a fully deuterated ligand environment that greatly suppresses multiphonon nonradiative deactivation pathways through avoidance of high-energy oscillators and rigidification of the ligand backbone. Strong luminescence is observed in CD_3CN for all four lanthanoids. Luminescence lifetimes in CD_3CN are among the highest values for molecular complexes in solution reported so far (Yb, τ_{obs} = 79 μs; Nd, τ_{obs} = 3.3 μs). For the ytterbium cryptate, the highest luminescence lifetime can be obtained using CD_3OD (τ_{obs} = 91 μs) and even in nondeuterated CH_3CN the lifetime is still unusually high (τ_{obs} = 53 μs). X-ray crystallography and ^{1}H NMR analysis of the corresponding nondeuterated lutetium cryptate suggest that the inner coordination sphere in solution is completely saturated by the octadentate cryptand and one chloride counterion. All lanthanoid cryptates remarkably show complete stability during reversed-phase HPLC measurements under strongly acidic conditions.

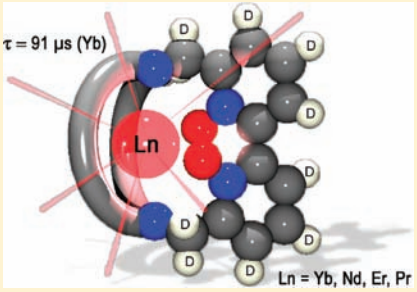

INTRODUCTION

Lanthanoid luminescence has received a lot of attention over the past decades due to the unique photophysical properties of Ln(III) ions, including element-specific luminescence, long luminescence lifetimes, and resistance to photobleaching. For several reasons Ln(III) ions emitting in the near-IR range are of considerable interest, as several emission bands fall within the range of known telecommunication windows (e.g., Nd^{3+}, Er^{3+}, Pr^{3+}) and because near-IR radiation (ca. 700−1100 nm) shows sizable penetration depth into biological tissue (Yb^{3+}, Nd^{3+}).[1] Thus, near-IR-emitting lanthanoids are an attractive or even indispensable component for various applications, such as light up- or downconverting systems[2] or biomedical luminescent probes.[1b−e] Near-IR-emitting lanthanoids, however, are prone to luminescence quenching by multiphonon relaxation processes. This phenomenon is especially severe with molecular complexes in solution, where the most detrimental high-energy oscillators (e.g., O−H, N−H, C−H) are usually ubiquitous and close to the metal center. One of the most crucial challenges for molecular, near-IR-emitting lanthanoid complexes is removal of highly quenching but inevitably present C−H groups ($\nu_{C-H} \approx 3000$ cm^{-1}) in the ligands. In the past, two strategies of fluorination ($\nu_{C-F} \approx 1200$ cm^{-1}) or deuteration ($\nu_{C-D} \approx 2200$ cm^{-1}) have been used to alleviate this problem.[3] Perfluorination promises more efficient suppression of vibrational quenching compared to perdeuteration due to the lower energy of the C−F stretching vibration but cannot be applied to many successful ligand systems for lanthanoids (e.g., amino carboxylates, DOTA derivates, cryptates) because of the chemical instability of the hypothetical, perfluorinated species in almost all instances. Therefore, perfluorinated ligands can only feature architectures with low denticities (e.g., acetylacetonates, imidodiphosphinates),[4] which can compromise complex stability under challenging conditions. Substitution of hydrogen against deuterium, on the other hand, allows adaptation of virtually all promising ligand systems for perdeuteration without substantially altering the photophysical properties. Many examples of highly near-IR-luminescent lanthanoid complexes have been reported in the recent past,[1,4−6] many of them involving fluorinated and/or deuterated ligands.

Cryptands based on bipyridine units are known to act as antenna moieties for sensitization of the near-IR emissive lanthanoids Yb and Nd.[7] In this context, we recently reported a series of deuterated isotopologues of the prototypical Lehn cryptate **Ln-1**[8] (Figure 1) for quantification of C−H quenching in the corresponding Yb and Nd species.[9]

The perdeuterated ytterbium analogue of **Ln-1**, however, showed only mediocre luminescence efficiency, probably due to the flexible nature of the cryptand and incomplete shielding of the metal center from solvent molecules. It has been reported[7b] in the past that ytterbium luminescence can be improved relative to **Ln-1** by slightly modifying the cryptand with one *N,N′*-bipyridine dioxide unit (**Ln-2**[10] in Figure 1). Here, we report the synthesis of the perdeuterated cryptates $[\mathbf{D_{30}}]$**-Ln-2** with the lanthanoids Yb, Nd, Er, Pr, and Lu and the corresponding structural and photophysical properties.

Received: November 2, 2011
Published: April 3, 2012

   dx.doi.org/10.1021/ic202376k | *Inorg. Chem.* 2012, 51, 4539−4545

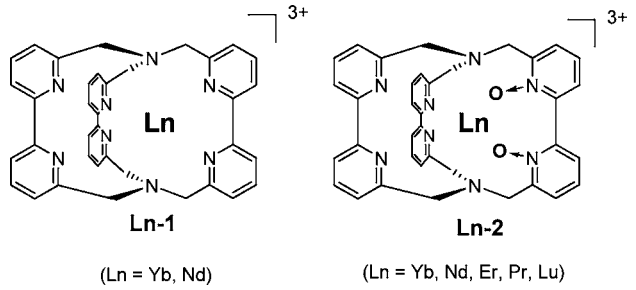

Figure 1. Tris(bipyridine)-derived lanthanoid cryptates **Ln-1** and **Ln-2**.

Scheme 1. Synthesis of the Perdeuterated Lanthanoid Cryptates $[D_{30}]$-Ln-2 (Ln = Yb, Nd, Er, Pr, Lu)

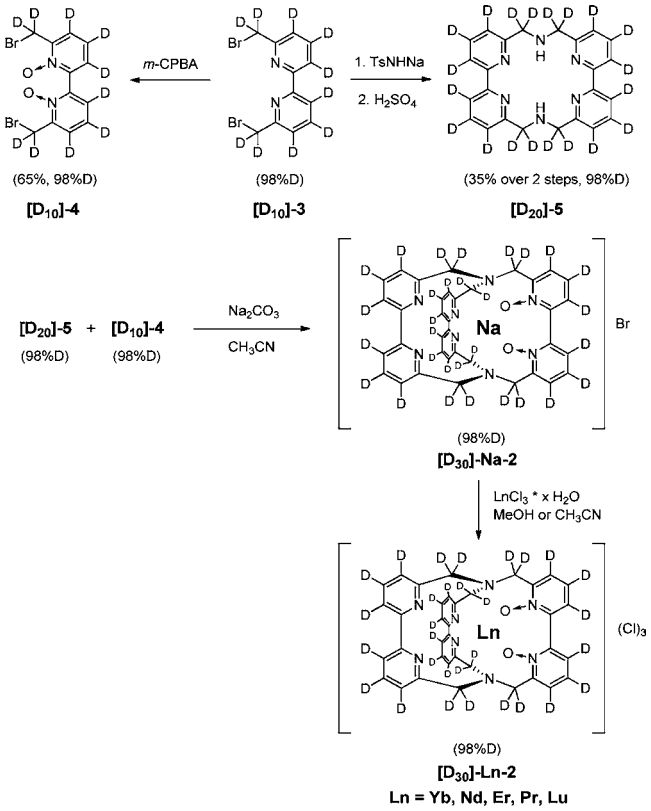

RESULTS AND DISCUSSION

Synthesis of the Lanthanoid Cryptates. Synthesis of the cryptates $[D_{30}]$-**Ln-2** (Scheme 1) was straightforward starting from building block $[D_{10}]$-**3**, which can be prepared very cost efficiently using D_2O as a cheap deuterium source.[9] All further transformations toward $[D_{30}]$-**Ln-2** did not necessitate any deuterated solvents and/or reagents and still allowed very high final deuteration levels of 98%D (see Figure S1 in the Supporting Information). In addition to the perdeuterated species, the nondeuterated cryptate **Lu-2** was also synthesized from the corresponding, known sodium cryptate **Na-2**.[10] The lanthanoid cryptates are highly soluble in polar, protic solvents like H_2O and MeOH, moderately in polar, nonprotic solvents like CH_3CN or DMF, and virtually insoluble in rather unpolar media like CH_2Cl_2 or toluene.

It is known that similar cryptates usually are very stable and kinetically inert.[7,11] Each cryptate $[D_{30}]$-**Ln-2** exhibits high complex stability owing to the macrobicyclic nature of the ligand. After days, no sign of decomposition was observed in common solvents. Conveniently, the purity of these cryptates can also be analyzed by reversed-phase HPLC using an acidic H_2O/CH_3CN gradient (Figure 2, see also Figures S2–S7 in the

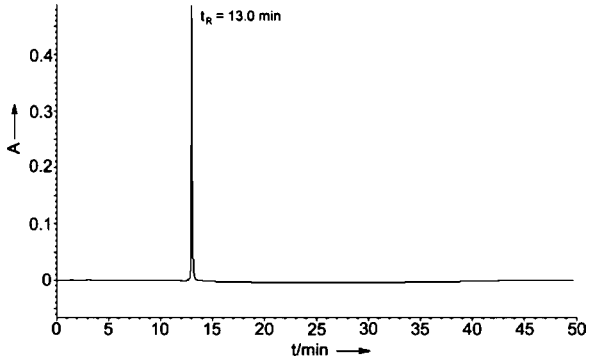

Figure 2. Complete stability under HPLC conditions: Chromatogram of $[D_{30}]$-**Yb-2** (Lichrospher RP-18e 125 mm × 4 mm-5 μm; eluents, H_2O + 1%TFA/CH_3CN → ~pH 1), UV detection at 300 nm).

Supporting Information). In this context, introduction of the bipyridine-*N,N'*-dioxide unit is sufficient to guarantee complete complex stability of the cryptates **Ln-2** even with the smaller lanthanoids Er, Yb, and Lu. This is in contrast to the corresponding tris(bipyridine) cryptates **Ln-1** (Figure 1: Ln = Er, Yb, Lu) which show considerable decomplexation under the same conditions.[9]

Structural Properties of the Lanthanoid Cryptates. Crystals suitable for single-crystal X-ray analysis were obtained from methanolic solutions of the nondeuterated cryptate **Lu-2**. The structure shows a 9-coordinate lutetium center with overall C_2 complex symmetry (Figure 3). Most importantly, the inner coordination sphere does not contain any solvent molecules

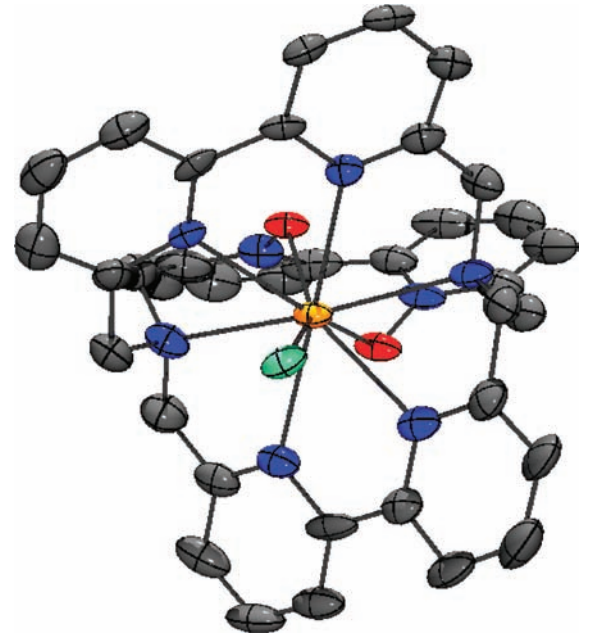

Figure 3. Lu-2. Thermal ellipsoid plot for the cation of **Lu-2** (Ortep 3 for Windows,[12] 50% probability level). Hydrogen atoms and free chloride anions are omitted for clarity. Color scheme: C, gray; N, blue; O, red; Cl, turquoise; Lu, orange.[13]

dx.doi.org/10.1021/ic202376k | Inorg. Chem. 2012, 51, 4539–4545

that could strongly quench near-IR lanthanoid luminescence (like H_2O or MeOH) but is instead completed by one of the chloride counteranions.

Structural characterization in solution was also possible on the diamagnetic cryptate **Lu-2**. ^{1}H NMR spectroscopy in CD_3OD clearly shows the presence of one single, C_2-symmetric species (Figure 4). Most of the very sharp signals are well

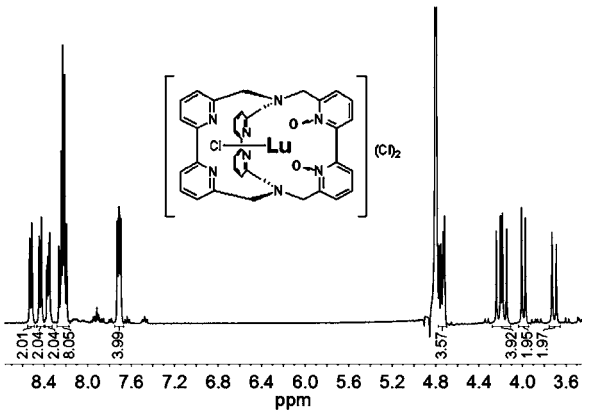

Figure 4. ^{1}H NMR spectrum of **Lu-2** (400 MHz, CD_3OD).

resolved and do not exhibit any signs of exchange broadening, e.g., all benzylic protons show sharp doublets with geminal coupling constants (12 Hz < ^2J < 16 Hz), which is consistent with the solid state structure where a chloride is bound to Lu.

This interpretation is also supported by the absence of inner-sphere methanol molecules as determined by luminescence lifetime measurements on the structurally closely related ytterbium cryptate [$\mathbf{D_{30}}$]-**Yb-2** in CH_3OH and CD_3OD (vide infra). The alternative, dissociation of the chloride anion upon dissolution and subsequent fast solvent/anion exchange is less probable in light of these observations. The situation seen for the lutetium cryptate is very likely also valid for the late lanthanoids Er and Yb because of the very similar ionic radii compared to Lu. The same assumption also seems reasonable for the bigger lanthanoids Pr and Nd due to the very limited possibilities for structural variation in the very rigid cryptates, but a definitive answer to this question for these lanthanoids remains unclear so far.

Photophysical Properties. [$\mathbf{D_{30}}$]-**Ln-2** (Ln = Yb, Nd, Er, Pr) in CD_3CN all exhibit very similar absorption band shapes (see Figure S8 in the Supporting Information) between 300 and 350 nm, which is a typical range for bipyridine-based cryptates. The absolute maxima shift slightly from λ_{max} = 305 nm for the early lanthanoids Pr and Nd to λ_{max} = 304 nm for the late lanthanoids Er and Yb. Steady state emission spectra of [$\mathbf{D_{30}}$]-**Ln-2** in the same solvent show strong near-IR luminescence with the characteristic bands for the lanthanoids Yb, Nd, Er, and Pr after excitation at λ_{exc} = 304 nm (Figure 5).

The emission spectrum of the complex [$\mathbf{D_{30}}$]-**Lu-2** at low temperature shows a structured band around 340 nm (residual intraligand singlet emission) and a broad, featureless band at lower energy (λ_{max} = 531 nm), which was assigned as the corresponding triplet emission (Figure 6) in analogy to similar cryptates.[14] The complete lack of vibrational structure of the latter band makes the exact determination of the zero-phonon $T_1 \rightarrow S_0$ transition energy $E(T_1)$ by fitting procedures quite arbitrary. A reasonable estimate, however, of the possible range is $E(T_1) \approx 20\,600-20\,000$ cm^{-1} (485−500 nm), which is

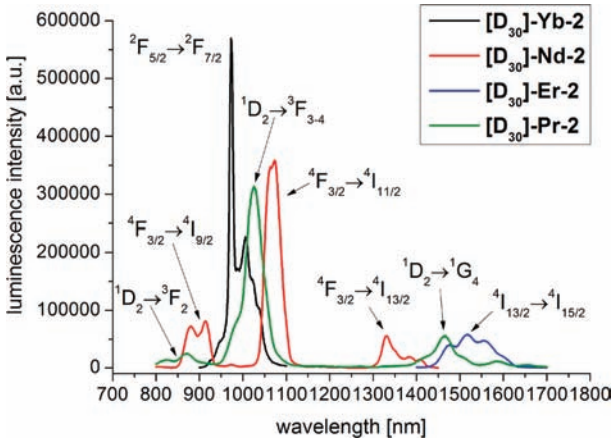

Figure 5. Steady state emission spectra of [$\mathbf{D_{30}}$]-**Ln-2** (Ln = Yb, Nd, Er, Pr) in CD_3CN (λ_{exc} = 304 nm; bandwidths Yb 4.0 nm, Nd 8.0 nm, Er/Pr 14.0 nm).

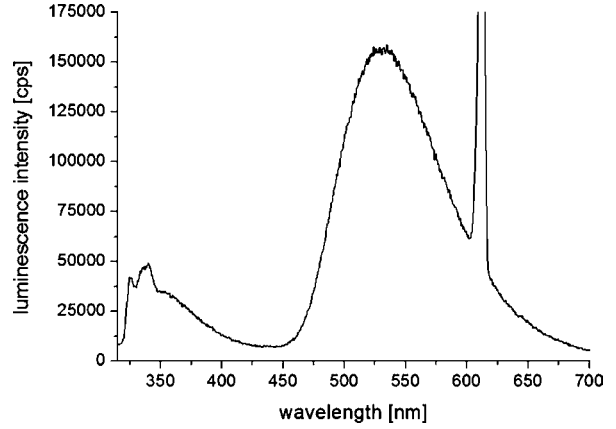

Figure 6. Low-temperature (77 K) steady state emission spectrum of [$\mathbf{D_{30}}$]-**Lu-2** (MeOH/EtOH, 1:1, v/v) (λ_{exc} = 304 nm; bandwidth 2.4 nm, second order excitation peak at ca. 608 nm).

comparable with previously reported estimates on **Gd-2** of $E(T_1) \approx 20\,500$ cm^{-1}.[14a] Interestingly, the triplet energy for the bipyridine-*N*,*N*′-dioxide cryptand in **Ln-2** is considerably lower than the one in the corresponding tris(bipyridine) cryptate **Gd-1** ($E(T_1)$ = 21 600 cm^{-1}).[14b]

The position of the triplet level in [$\mathbf{D_{30}}$]-**Ln-2** seems especially appropriate for the efficient direct population of the $^1D_2$ level (ca. 16 800 cm^{-1})[15] of Pr(III) by the usually operative energy transfer mechanism. In contrast, the $^3P_0$ level (ca. 20 700 cm^{-1})[15] lies too close to the triplet level to prevent energy backtransfer onto the ligand and concomitant loss of sensitization efficiency. Consequently, the steady state emission spectrum of [$\mathbf{D_{30}}$]-**Pr-2** shows strong bands involving the $^1D_2$ term as the initial level, while transitions originating from $^3P_0$ are not observed (Figure 5). Population of the emissive states of Nd ($^4F_{3/2}$ at ca. 11 500 cm^{-1})[15] and Er ($^4I_{13/2}$ at ca. 6600 cm^{-1})[15] is likely to occur by initial energy transfer from the ligand-centered triplet state to available high-lying lanthanoid energy levels followed by nonradiative transitions to the respective emitting levels. In the case of Yb, this mechanism is not possible because of the availability of only one single excited energy level ($^2F_{5/2}$ at ca. 10 250 cm^{-1}). The large energy difference between this state and the cryptand triplet state implies that the energy transfer described for Pr, Nd, and Er

dx.doi.org/10.1021/ic202376k | Inorg. Chem. 2012, 51, 4539−4545

cannot be very efficient. While the exact sensitization mechanism for $[D_{30}]$-**Yb-2** remains unclear at this moment, it could be connected to an electron-transfer-mediated process which has been invoked in various ytterbium complex architectures,[1c,d] including bipyridine-based cryptates.[7c]

Luminescence lifetime measurements in CD_3CN gave monoexponential decay kinetics for $[D_{30}]$-**Yb-2** and $[D_{30}]$-**Nd-2**, while the fitting of the decay profile for $[D_{30}]$-**Er-2** gave significantly better results with a biexponential approach (Table 1, see Figures S9–S11 in the Supporting Information). For all

Table 1. Luminescence Lifetimes τ_{obs} for $[D_{30}]$-Ln-2 in CD_3CN (λ_{exc} = 304 nm)

entry	Ln	τ_{obs}[a] [μs]	transition
1	Yb	79	$^2F_{5/2} \rightarrow {}^2F_{7/2}$ (975 nm)
2	Nd	3.3	$^4F_{3/2} \rightarrow {}^4I_{11/2}$ (1075 nm)
3	Er	5.7 (34%)	$^4I_{13/2} \rightarrow {}^4I_{15/2}$ (1550 nm)
		1.8 (66%)	

[a]Estimated uncertainties in τ_{obs} are ±10% for Yb and ±15% for Nd and Er.

three lanthanoids, no rise times were observed. The lifetime for the cryptate $[D_{30}]$-**Pr-2** was expectedly too short (τ_{obs} < ca. 0.8 μs) to be reliably measurable with our instrumentation.

The lifetimes for the Yb, Nd, and Er cryptates are all among the best values for molecular complexes with the respective lanthanoid in solution reported so far. Rough estimates of the intrinsic quantum yields $\Phi_{Ln}^{Ln} = \tau_{obs}/\tau_{rad}$ of Yb and Nd using typical values for the radiative lifetimes τ_{rad} (Yb, $\tau_{rad} \approx 1.2-1.3$ ms; Nd, $\tau_{rad} \approx 0.2-0.5$ ms)[1a] give rather high values (Yb ≈ 6.1–6.6%; Nd ≈ 0.66–1.7%).

Because of the especially remarkable intrinsic luminescence efficiency of the ytterbium cryptate, further measurements were conducted for $[D_{30}]$-**Yb-2** in order to assess several photophysical parameters determining the emission efficiency. Absorption and emission spectra were collected in the three additional solvents CH_3CN, CD_3OD, and CH_3OH (Figure 7).

The absorption spectra (Figure 7, left column) do not show significant differences, neither with the variation of the nature of the solvent nor with the isotopologic composition within one

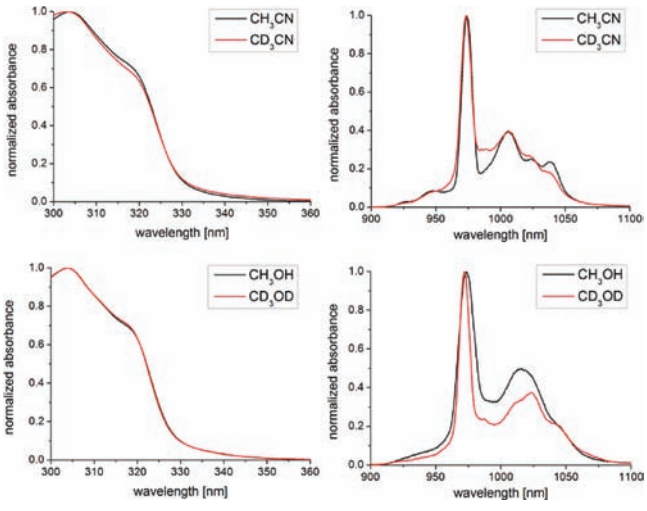

Figure 7. Normalized absorption (left column) and emission spectra (right column, λ_{exc} = 304 nm) of $[D_{30}]$-**Yb-2** in CD_3CN/CH_3CN (upper row) and CD_3OD/CH_3OH (lower row).

solvent class (methanol or acetonitrile). In the emission spectra, however, clear differences are evident (Figure 7, right column). Especially striking are the changes in the band shapes upon deuteration of either of the two solvents (methanol or acetonitrile). The reason for this phenomenon remains unclear at this point.

Luminescence lifetimes were measured in CH_3CN in order to assess the influence of solvent deuteration (Table 2). In

Table 2. Luminescence Lifetimes τ_{obs} for $[D_{30}]$-Yb-2 in Organic Media (λ_{exc} = 304 nm, λ_{em} = 975 nm)

entry	solvent	τ_{obs}[a] [μs]
1	CD_3CN	79
2	CD_3OD	91
3	CH_3CN	53
4	CH_3OH	14

[a]Estimated uncertainties in τ_{obs} are ±10%.

addition, the measurements in CD_3OD and CH_3OH were performed to determine the number of inner-sphere solvent molecules in solution (Table 2, Figure 8).

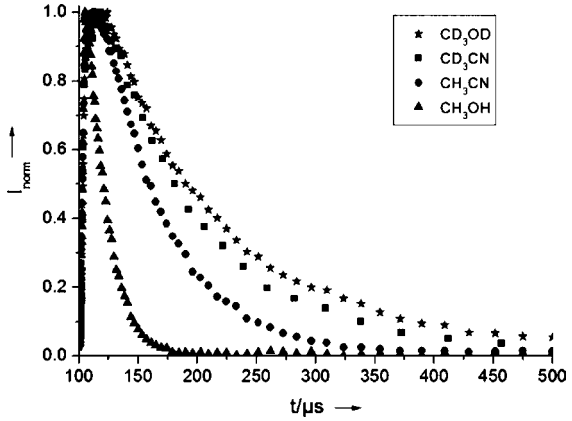

Figure 8. Luminescence decay profiles of the ytterbium cryptate $[D_{30}]$-**Yb-2** in different solvents (λ_{exc} = 304 nm, λ_{em} = 975 nm).

All luminescence decays (Figure 8) were found to be monoexponential (see Figures S11–S14 in the Supporting Information). The lifetimes in the perdeuterated solvents CD_3OD and CD_3CN are exceptionally long (Table 2, entries 1 + 2: τ_{obs} = 79 μs in CD_3CN and τ_{obs} = 91 μs in CD_3OD), and even nondeuterated CH_3CN results in unusually slow decay kinetics (Table 2, entry 3: τ_{obs} = 53 μs). The lifetime differences in CH_3OH (τ_{obs} = 14 μs, Table 2, entry 4) and CD_3OD (τ_{obs} = 91 μs, Table 2, entry 2) allow estimation of the number of inner-sphere methanol molecules (q_{MeOH}) with the empirical equation developed by Beeby et al.[16] The obtained value of almost zero (q_{MeOH} = −0.08) suggests that the structure in solution is the same as that seen in the crystal structure of **Lu-2** (vide supra). The differences between the lifetimes in deuterated and nondeuterated methanol can therefore be assigned entirely to second and outer-sphere quenching contributions. The absence of inner-sphere methanol molecules, in conjunction with the complete absence of high-energy X–H oscillators (X = O, N, C) in the perdeuterated cryptate and together with the very rigid nature of the ligand environment, helps explain the great luminescence efficiencies of $[D_{30}]$-**Ln-2**.

dx.doi.org/10.1021/ic202376k | Inorg. Chem. 2012, 51, 4539–4545

CONCLUSION

We developed highly luminescent, molecular NIR-emitting lanthanoid complexes with Yb, Nd, Er, and Pr by perdeuterating the macrobicyclic, rigid cryptate architecture **Ln-2**. In the case of ytterbium, this architecture leads to outstanding minimization of nonradiative deactivation processes and exceptionally efficient sensitization of lanthanoid luminescence, which is reflected in very long luminescence lifetimes in two deuterated solvents (CD_3CN and CD_3OD) and even in nondeuterated CH_3CN. The lifetime values for the lanthanoids Yb, Nd, and Er are among the best values reported so far. In addition, [$\mathbf{D_{30}}$]-**Ln-2** shows remarkable resistance toward decomplexation in solution, even under conditions where other lanthanoid complexes would quickly decompose. The extraordinary luminescence efficiency combined with the high complex stability make [$\mathbf{D_{30}}$]-**Ln-2** quite unique among NIR luminophores. The successful design exemplified by [$\mathbf{D_{30}}$]-**Ln-2** opens very promising new avenues for realization of bright and robust lanthanoid luminophores in the near-IR region.

EXPERIMENTAL SECTION

General. Chemicals were purchased from commercial suppliers and used as received unless stated otherwise. Deuterated solvents had deuterium contents > 99.8% D and were used as commercially available without additional purification or drying procedures. CH_3CN for the synthesis of the cryptates was HPLC grade. Other solvents were dried by standard procedures (EtOH: Mg/I_2). Air-sensitive reactions were carried out under a dry, dioxygen-free atmosphere of N_2 using the Schlenk technique. Column chromatography was performed with silica gel 60 (Merck, 0.063−0.200 mm). Analytical thin layer chromatography (TLC) was done on silica gel 60 F_{254} plates (Merck, coated on aluminum sheets). Overall deuteration levels were established by deconvolution of the corresponding mass spectra. ESI mass spectrometry was done using Bruker Daltonics Esquire6000. NMR spectra were measured on a Bruker DPX-250 (^{1}H, 250 MHz; ^{13}C, 62.9 MHz) or a Bruker DRX-400 (^{1}H, 400 MHz; ^{13}C, 101 MHz). UV−vis spectra were recorded on a Jasco-670 spectrophotometer using 1.0 cm quartz cuvettes. The purity of the lanthanoid cryptates was checked by analytical reversed-phase HPLC (Lichrospher RP-18e, 125 × 4 mm-5 μm; flow rate, 1 mL min^{-1}; UV detection, 300 nm). The only major impurity occasionally observed in the lanthanoid complexes was the corresponding sodium cryptate. The presence of the sodium cryptate can easily be detected by HPLC, whereas elemental analysis was not always suitable to rule out this contaminant.

Photophysical Measurements. Steady state emission spectra were acquired on a PTI Quantamaster QM4 spectrofluorimeter using 1.0 cm quartz cuvettes at room temperature. All solvents (CD_3OD/CD_3CN, NMR grade 99.8% D; CH_3OH/CH_3CN, analytical grade) were purchased from commercial suppliers and used as received without special drying procedures. The excitation light source was a 75 W continuous xenon short arc lamp. Emission was monitored at 90° using a PTI P1.7R detector module (Hamamatsu PMT R5509-72 with a Hamamatsu C9525 power supply operated at −1500 V and a Hamamatsu liquid N_2 cooling unit C9940 set to −80 °C). For the near-IR steady state emission measurements at room temperature, a long-pass filter RG-780 (Schott, 3.0 mm thickness, transmission > 83% between 800 and 850 nm and > 99% between 850 and 1700 nm) was used in the emission channel in order to avoid higher order excitation light. Low-temperature spectra were recorded on frozen glasses of solutions of [$\mathbf{D_{30}}$]-**Lu-2** (MeOH/EtOH 1:1, v/v) using a Dewar cuvette filled with liquid N_2 (T = 77 K). Spectral selection was achieved by single-grating monochromators (excitation, 1200 grooves/mm, blazed at 300 nm; visible emission, 1200 grooves/mm, blazed at 400 nm; near-IR emission, 600 grooves/mm, blazed at 1200 nm). Luminescence lifetimes were determined with the same instrumental setup. No long-pass filter was used. The light source for these measurements was a xenon flash lamp (Hamamatsu L4633, 10 Hz repetition rate; pulse width, ca. 1.5 μs fwhm). Lifetime data analysis (deconvolution, statistical parameters, etc.) was performed using the software package FeliX32 from PTI. Lifetimes were either determined by fitting the middle and tail portions of the decays or by deconvolution of the decay profiles with the instrument response function which was determined using a dilute aqueous dispersion of colloidal silica (Ludox AM-30). The estimated uncertainties in τ_{obs} are ±10% for all Yb cryptates and ±15% for Er and Nd. All measured values are averages of three independent experiments.

X-ray Analysis. A colorless needle of **Lu-2** having approximate dimensions of 0.41 × 0.16 × 0.13 mm^3 was mounted on a glass fiber using perfluoropolyether oil. The measurement was carried out on an Oxford Xcalibur 2 diffractometer using monochromated Mo Kα radiation. Data were collected at a temperature of 107.5(2) K. Frames corresponding to an arbitrary hemisphere of data were collected using ω scans. The structure was solved within the Wingx[17] package using direct methods (SIR92[18]) and expanded using Fourier techniques (SHELXL-97[19]). Hydrogen atoms were included but not refined. They were positioned geometrically, with distances C−H = 0.93 Å for aromatic hydrogens and C−H = 0.97 Å in all benzylic positions. All hydrogens were constrained to ride on their parent carbon atoms. U_{iso}(H) values were set at 1.2 times U_{eq}(C). The unit cell contains voids with highly disordered solvent molecules. The residual electron density as well as the volume suggest the presence of one methanol and one diethyl ether molecule per formula unit. These solvents were treated as diffuse contribution to the scattering without assignment of precise positional parameters by the SQUEEZE routine of PLATON.[20]

Synthesis of [$\mathbf{D_{10}}$]-4.[10] With cooling in an ice bath, a solution of *m*-chloroperbenzoic acid (moistened → 77 wt %, 210 mg, 0.94 mmol, 2.6 equiv) in $CHCl_3$ (10 mL) was added dropwise to a solution of [$\mathbf{D_{10}}$]-**3**[9] (98% D, 127 mg, 0.36 mmol, 1.0 equiv) in $CHCl_3$ (25 mL). The mixture was allowed to come to room temperature, and at 24 h intervals equal portions of *m*-chloroperbenzoic acid were added with ice bath cooling (5 × 210 mg). The reaction mixture was washed with saturated, aqueous $NaHCO_3$ (10 × 80 mL). The organic layer was dried ($MgSO_4$) and concentrated in vacuo. The slightly yellow crude product was purified by column chromatography (SiO_2, CH_2Cl_2/MeOH 50:1, UV detection, preloading onto SiO_2), giving a white solid. The solid was dissolved in $CHCl_3$; the organic layer was washed with saturated $NaHCO_3$ (5 × 70 mL) and dried over $MgSO_4$. Solvent was removed in vacuo, yielding the product as a white solid. Yield: 90 mg (65%; overall deuteration level, 98% D). MS (ESI$^+$): m/z (%) = 406.92 (95, [M + Na]$^+$), 422.88 (53, [M + K]$^+$). TLC: R_f = 0.46 (SiO_2, CH_2Cl_2/MeOH 9:1, UV detection).

Synthesis of [$\mathbf{D_{20}}$]-5.[21] Under N_2, [$\mathbf{D_{10}}$]-**3**[9] (98% D, 1.03 g, 2.91 mmol, 1.0 equiv) was dissolved in dry EtOH (90 mL) and TsNHNa[22] (1.13 g, 5.83 mmol, 2.0 equiv) was added. The mixture was heated under reflux for 40 h. The white suspension was cooled in an ice bath for 1 h; the colorless solid was collected and washed with cold water and EtOH. After drying in vacuo, the product was obtained as a colorless solid (0.72 g). The crude ditosylate (0.72 g, 1.0 mmol) was dissolved in concentrated H_2SO_4 (10 mL) and heated to 110 °C (bath temperature) for 3 h. The cold solution was poured onto crushed ice (ca. 30 g), and aqueous NaOH (30 wt %) was added until pH > 13. The turbid suspension was extracted with $CHCl_3$ (4 × 100 mL); the combined organic phases were dried ($MgSO_4$) and concentrated to yield an off-white solid (0.42 g, 35% over 2 steps, overall deuteration level 98% D). This material was used without further purification. MS (ESI$^+$): m/z (%) = 415.21 (10, [M + H]$^+$), 437.14 (100, [M + Na]$^+$).

Synthesis of [$\mathbf{D_{30}}$]-Na-2. Under N_2, a solution of [$\mathbf{D_{20}}$]-**5** (98% D, 97 mg, 0.234 mmol, 1.0 equiv), [$\mathbf{D_{10}}$]-**4** (98% D, 90 mg, 0.234 mmol, 1.0 equiv), and Na_2CO_3 (248 mg, 2.34 mmol, 10 equiv) in CH_3CN (100 mL, HPLC grade) was heated under reflux for 60 h. The reaction mixture was filtered warm, the filtrate was concentrated, and the residue was subjected to column chromatography (SiO_2, CH_2Cl_2/MeOH gradient 24:1 → 9:1, UV detection, staining with I_2 vapor, preloading onto SiO_2) giving the product as a white solid. Yield: 63 mg (36%; overall deuteration level, 98% D; see Figure S1 in the Supporting Information). ^{13}C NMR (62.9 MHz, CD_2Cl_2): δ = 159.1,

dx.doi.org/10.1021/ic202376k | Inorg. Chem. 2012, 51, 4539−4545

158.3, 157.6, 157.0, 148.4, 145.6, 138.6−137.5 (m, 2 C), 129.6−128.8 (m, 1 C), 127.2−126.4 (m, 1 C), 125.0−124.2 (m, 3 C), 122.6−121.0 (m, 2 C), 61.4−60.0 (m, 2 C), 54.6−53.8 (m, 1 C) ppm. MS (ESI^+): m/z (%) = 659.2 (100, $[M]^+$). TLC: R_f = 0.13 (SiO_2, CH_2Cl_2/MeOH 9:1, UV detection, staining with I_2 vapor).

Synthesis of [D_{30}]-Yb-2. Under N_2, the perdeuterated cryptate [D_{30}]-**Na-2** (98% D, 21 mg, 0.028 mmol, 1.0 equiv) was dissolved in MeOH (20 mL) and heated under reflux. $YbCl_3 \cdot 6\ H_2O$ (16 mg, 0.042 mmol, 1.5 equiv) was dissolved in MeOH (3 mL) and added to the refluxing solution. The reaction mixture was heated under reflux for 26 h. After cooling to room temperature, the solvent was removed in vacuo. The white solid was dissolved in a minimum amount of MeOH and layered with Et_2O until the solution became turbid. The mixture was stored at 4 °C overnight, and the precipitate was filtered over a nylon membrane filter (0.45 μm). The faintly pink solid was dried in vacuo. Yield: 14.6 mg. MS (ESI^+): m/z (%) = 843.05 ($[M + 2Cl]^+$).

Synthesis of [D_{30}]-Lu-2. Under N_2, the perdeuterated cryptate [D_{30}]-**Na-2** (98% D, 21 mg, 0.028 mmol, 1.0 equiv) was dissolved in MeOH (20 mL) and heated under reflux. $LuCl_3 \cdot 6\ H_2O$ (16 mg, 0.042 mmol, 1.5 equiv) was dissolved in MeOH (3 mL) and added to the refluxing solution. The reaction mixture was heated under reflux for 24 h. After cooling to room temperature, the solvent was removed in vacuo. The white solid was dissolved in a minimum amount of MeOH and layered with Et_2O until the solution became turbid. The mixture was stored at 4 °C overnight, and the precipitate was filtered over a nylon membrane filter (0.45 μm). The beige solid was dried in vacuo. Yield: 11 mg. MS (ESI^+): m/z (%) = 423.09 ($[M + Cl]^{2+}$).

Synthesis of [D_{30}]-Ln-2 (Ln = Nd, Er, Pr, Lu) and of Lu-2. The appropriate cryptate ([D_{30}]-**Na-2** or **Na-2**[10]) was dissolved in CH_3CN (ca. 0.25 mL per μmol of the sodium cryptate), and $LnCl_3 \cdot xH_2O$ (1.5 equiv, x = 6 for Ln = Nd, Er, Lu and x = 7 for Ln = Pr) was added. The mixture was heated under reflux for 40 h. The solvent was removed, and the residue was dissolved in a minimum amount of MeOH. The solution was layered with Et_2O until the mixture became turbid. After storing the mixture at 4 °C overnight, the precipitate was collected on a nylon membrane filter (0.45 μm), washed with Et_2O, and dried under reduced pressure. The complexes were obtained as colorless to light-green solids.

Lu-2. Yield: 16 mg of a colorless solid (from 15 mg of the sodium cryptate). ^1H NMR (400 MHz, CD_3OD): δ = 8.52 (d, J = 8.0 Hz, 2 H), 8.44 (d, J = 8.1 Hz, 2 H), 8.39−8.32 (m, 2 H), 8.29−8.17 (m, 8 H), 7.78−7.67 (m, 4 H), 4.75 (d, J = 15.3 Hz, 2 H), 4.73 (d, J = 12.8 Hz, 2 H), 4.22 (d, J = 15.8 Hz, 2 H), 4.16 (d, J = 15.3 Hz, 2 H), 3.99 (d, J = 12.8 Hz, 2 H), 3.71 (d, J = 15.8 Hz, 2 H) ppm. ^{13}C NMR (101 MHz, CD_3OD): δ = 159.1, 156.7, 155.9, 153.8, 150.8, 144.6, 142.9, 142.2, 136.1, 132.2, 130.9, 126.8, 126.4, 123.6, 123.2, 61.6, 60.2, 56.9 ppm. MS (ESI^+): m/z (%) = 408.06 ($[M + Cl]^{2+}$).

Single crystals were grown by vapor diffusion of Et_2O into a solution of the compound in CH_3OH.

[D_{30}]-Nd-2. Yield: 7.3 mg of a colorless solid (from 12 mg of the sodium cryptate). MS (ESI^+): m/z (%) = 407.72 ($[M + Cl]^{2+}$).

[D_{30}]-Er-2. Yield: 15 mg of a colorless solid (from 12 mg of the sodium cryptate). MS (ESI^+): m/z (%) = 419.20 ($[M + Cl]^{2+}$).

[D_{30}]-Pr-2. Yield: 8.3 mg of a light-green solid (from 11 mg of the sodium cryptate). MS (ESI^+): m/z (%) = 406.17 ($[M + Cl]^{2+}$).

■ ASSOCIATED CONTENT

Ⓢ Supporting Information

ESI mass spectrum for [D_{30}]-**Na-2**, UV−vis spectra for [D_{30}]-**Ln-2** (Ln = Yb, Nd, Er, Pr) in CD_3CN, HPLC traces for the lanthanoid cryptates, luminescence decay profiles for [D_{30}]-**Ln-2** (Ln = Yb, Nd, Er), crystallographic information file for **Lu-2**. This material is available free of charge via the Internet at http://pubs.acs.org.

■ AUTHOR INFORMATION

Corresponding Author

*E-mail: michael.seitz@rub.de.

Notes

The authors declare no competing financial interest.

■ ACKNOWLEDGMENTS

C.D. and M.M. are grateful for support by the Ruhr-University Research School. M.S. thanks Prof. Dr. Nils Metzler-Nolte (Ruhr-University Bochum) for his continued support. The authors thank Prof. Dr. Roland A. Fischer for access to the diffractometer and Dr. Klaus Merz for help with the crystal structure refinement. Financial support is gratefully acknowledged from DFG (Emmy Noether Fellowship M.S.), Fonds der Chemischen Industrie (Liebig Fellowship M.S. and predoctoral fellowships C.D., for N.A. and M.M.), and Research Department Interfacial Systems Chemistry (Ruhr-University Bochum).

■ REFERENCES

(1) (a) Bünzli, J.-C. G.; Eliseeva, S. V. In *Lanthanide Luminescence (Springer Series on Fluorescence 7)*; Hänninen, P., Härma, H., Eds.; Springer: Berlin, 2011; pp 1−45. (b) Werts, M. H. V. In *Lanthanide Luminescence (Springer Series on Fluorescence 7)*; Hänninen, P., Härma, H., Eds.; Springer: Berlin, 2011; pp 133−160. (c) Bünzli, J.-C. G.; Eliseeva, S. V. *J. Rare Earths* **2010**, *28*, 824−842. (d) Comby, S.; Bünzli, J.-C. G. In *Handbook on the Physics and Chemistry of Rare Earths*; Gschneidner, K. A., Jr., Bünzli, J.-C. G., Pecharsky, V. K., Eds.; Elsevier: Amsterdam, 2007; Vol. *37*, pp 217−470. (e) Faulkner, S.; Pope, S. J. A.; Burton-Pye, B. P. *Appl. Spectrosc. Rev.* **2005**, *40*, 1−31.

(2) (a) Haase, M.; Schäfer, H. *Angew. Chem., Int. Ed.* **2011**, *50*, 5808−5829. (b) van der Ende, B. M.; Aarts, L.; Meijerink, A. *Phys. Chem. Chem. Phys.* **2009**, *11*, 11081−11095. (c) Wang, F.; Liu, X. *Chem. Soc. Rev.* **2009**, *38*, 976−989.

(3) (a) Browne, W. R.; Vos, J. G. *Coord. Chem. Rev.* **2001**, *219−221*, 761−787. (b) Yanagida, S.; Hasegawa, Y.; Murakoshi, K.; Wada, Y.; Nakashima, N.; Yamanaka, T. *Coord. Chem. Rev.* **1998**, *171*, 461−480.

(4) (a) Kishimoto, S.; Nakagawa, T.; Kawai, T.; Hasegawa, Y. *Bull. Chem. Soc. Jpn.* **2011**, *84*, 148−154. (b) Glover, P. B.; Bassett, A. P.; Nockemann, P.; Kariuki, B. M.; Van Deun, R.; Pikramenou, Z. *Chem.—Eur. J.* **2007**, *13*, 6308−6320. (c) Sung, L.-N.; Yu, J.-B.; Zheng, G.-L.; Zhang, H.-J.; Meng, Q.-G.; Peng, C.-Y.; Fu, L.-S.; Liu, F.-Y.; Yu, Y.-N. *Eur. J. Inorg. Chem.* **2006**, 3962−3973. (d) Kim, J.-H.; Park, Y.-P. *J. Korean Phys. Soc.* **2003**, *43*, 277−281. (e) Hasegawa, Y.; Ohkubo, T.; Sogabe, K.; Kawamura, Y.; Wada, Y.; Nakashima, N.; Yanagida, S. *Angew. Chem., Int. Ed.* **2000**, *39*, 357−360.

(5) (a) Hebbink, G. A.; Reinhoudt, D. N.; van Veggel, F. C. J. M. *Eur. J. Org. Chem.* **2001**, 4101−4106. (b) Tsvirko, M. P.; Meshkova, S. B.; Venchikov, V. Y.; Topilova, Z. M.; Bol'shoi, D. V. *Opt. Spectrosc.* **2001**, *90*, 669−673. (c) Beeby, A.; Clarkson, I. M.; Dickins, R. S.; Faulkner, S.; Parker, D.; Royle, L.; de Sousa, A. S.; Williams, J. A. G.; Woods, M. *J. Chem. Soc., Perkin Trans. 2* **1999**, 493−503. (d) Wolbers, M. P. O; van Veggel, F. C. J. M.; Snellink-Ruël, B. H. M.; Hofstraat, J. W.; Geurts, F. A. J.; Reinhoudt, D. N. *J. Chem. Soc., Perkin Trans. 2* **1998**, 2141−2150.

(6) (a) He, H.; Si, L.; Zhong, Y.; Dubey, M. *Chem. Commun.* **2012**, *48*, 1886−1888. (b) Zhang, T.; Zhu, X.; Cheng, C. C. W.; Kwok, W.-M.; Tam, H.-L.; Hao, J.; Kwong, D. W. J.; Wong, W.-K.; Wong, K.-L. *J. Am. Chem. Soc.* **2011**, *133*, 20120−20122. (c) Moore, E. G.; Xu, J.; Dodani, S.; Jocher, C. J.; D'Aleo, A.; Seitz, M.; Raymond, K. N. *Inorg. Chem.* **2010**, *49*, 4156−4166. (d) Shavaleev, N. M.; Scopelliti, R.; Gumy, F.; Bünzli, J.-C. G. *Inorg. Chem.* **2009**, *48*, 7937−7946. (e) Zhang, J.; Petoud, S. *Chem.—Eur. J.* **2008**, *14*, 1264−1272. (f) Jocher, C. J.; Moore, E. G.; Pierce, J. D.; Raymond, K. N. *Inorg. Chem.* **2008**, *47*, 7951−7953. (g) Zhang, J.; Badger, P. D.; Geib, S. J.; Petoud, S. *Angew. Chem., Int. Ed.* **2005**, *44*, 2508−2512.

(7) (a) Coldwell, J. B.; Felton, C. E.; Harding, L. P.; Moon, R.; Pope, S. J. A.; Rice, C. R. *Chem. Commun.* **2006**, 5048−5050. (b) Korovin, Y. V.; Rusakova, N. V.; Popkov, Y. A. *J. Appl. Spectrosc.* **2002**, *69*, 89−92.

(c) Faulkner, S.; Beeby, A.; Carrie, M.-C.; Dadabhoy, A.; Kenwright, A. M.; Sammes, P. G. *Inorg. Chem. Commun.* **2001**, *4*, 187−190.
(8) Alpha, B.; Lehn, J.-M.; Mathis, G. *Angew. Chem., Int. Ed.* **1987**, *26*, 266−267.
(9) Bischof, C.; Wahsner, J.; Scholten, J.; Trosien, S.; Seitz, M. *J. Am. Chem. Soc.* **2010**, *132*, 14334−14335.
(10) Lehn, J.-M.; Roth, C. O. *Helv. Chim. Acta* **1991**, *74*, 572−578.
(11) Mathis, G.; Bazin, H. In *Lanthanide Luminescence (Springer Series on Fluorescence 7)*; Hänninen, P., Härma, H., Eds.; Springer: Berlin, 2011; pp 47−88.
(12) Ortep-3 for Windows: Farrugia, L. J. *J. Appl. Crystallogr.* **1997**, *30*, 565.
(13) Crystallographic data for **Lu-2**: chemical formula $C_{36}H_{30}Cl_3LuN_8O_2{\cdot}MeOH{\cdot}Et_2O$, formula weight 994.16, T = 107.5 K, λ = 0.71073 Å, trigonal, space group $R\bar{3}$ (no. 148), $a = b$ = 37.0817(8), c = 16.1486(5), $\alpha = \beta = 90°$, $\gamma = 120°$, V = 19230.2(8) Å^3, Z = 18, μ = 2.548 mm^{-1}, $R(F_0)$ = 0.0601, $R_w(F_o^2)$ = 0.1798, GOF = 1.082.
(14) (a) Prodi, L.; Maestri, M.; Balzani, V.; Lehn, J.-M.; Roth, C. *Chem. Phys. Lett.* **1991**, *180*, 45−50. (b) Alpha, B.; Ballardini, R.; Balzani, V.; Lehn, J.-M.; Perathoner, S.; Sabbatini, N. *Photochem. Photobiol.* **1990**, *52*, 299−306.
(15) Energy levels of the trivalent lanthanoid aquo species: Carnall, W. T.; Fields, P. R.; Rajnak, K. *J. Chem. Phys.* **1968**, *49*, 4424−4442.
(16) Beeby, A.; Burton-Pye, B. P.; Faulkner, S.; Motson, G. R.; Jeffery, J. C.; McCleverty, J. A.; Ward, M. D. *J. Chem. Soc., Dalton Trans.* **2002**, 1923−1928.
(17) Wingx: Farrugia, L. J. *J. Appl. Crystallogr.* **1999**, *32*, 837−848.
(18) SIR92: Altomare, A.; Cascarano, G.; Giacovazzo, C.; Guagliardi, A. *J. Appl. Crystallogr.* **1993**, *26*, 343−350.
(19) Sheldrick, G. M. *SHELX97-Programs for Crystal Structure Analysis*; Institut für Anorganische Chemie der Universität Göttingen: Göttingen, Germany, 1998.
(20) Spek, A. L. *Acta Crystallogr.* **2009**, *D65*, 148−155.
(21) Newkome, G. R.; Pappalardo, S.; Gupta, V. K.; Fronczek, F. R. *J. Org. Chem.* **1983**, *48*, 4848−4851.
(22) Mekelburger, H.-B.; Groß, J.; Schmitz, J.; Nieger, M.; Vögtle, F. *Chem. Ber.* **1993**, *126*, 1713−1721.